Biomimetic tool design improves tillage efficiency, seedbed quality, and straw incorporation during rototilling in conservation farming

Ian Torotwa, Qishuo Ding, Emmanuel Awuah, Ruiyin He

College of Engineering, Nanjing Agricultural University, Key Laboratory of Intelligent Agricultural Equipment of Jiangsu Province, Nanjing, China

Abstract

Rotary tillage facilitates conservation agriculture in rice-based crop farming systems through minimal soil disturbance for seedbed preparation and crop residue management. However, efficiency of rotary tiller blades is hampered by degraded paddy soils and excessive crop residue conditions. Biomimetics presents an edge in the optimisation design of cultivation tools and can be employed to improve the efficiency of rotary tiller blades. This study was designed to evaluate the adaptability and performance of biomimetic rotary tiller blades inspired by the geometric structure of a mole rat's claw. Field experiments were conducted to evaluate the blades' torque and power requirements, soil fragmentation, displacement characteristics, and the rate of straw incorporation at three tillage depths (*i.e.*, 40, 70, and 100 mm). Results revealed that the biomimetic blades minimised torque by up to 21.05%, had lower specific power requirements, and produced finer tilths with granular and more even clod sizes than conventional blades. It also achieved more redistribution of topsoil and improved the straw burial rate. The biomimetic rotary tiller blades are thus energy-efficient and can improve soil structure and the quality of seedbeds, besides managing crop residues through incorporation, and therefore advance conservation tillage in intensive farming systems.

Correspondence: Ruiyin He, College of Engineering, Nanjing Agricultural University, Key Laboratory of Intelligent Agricultural Equipment of Jiangsu Province, Nanjing, 210031, China.
E-mail: ryhe@njau.edu.cn; iantorotwa@live.com

Key words: biomimetic design; conservation tillage; mean weight diameter; rotary tillage; straw incorporation; torque.

Received for publication: 19 December 2021.
Revision received: 10 May 2022.
Accepted for publication: 26 May 2022.

Journal of Agricultural Engineering 2023; LIV:1327
doi:10.4081/jae.2023.1327

Introduction

Soil tillage is an essential farming operation that creates workable seedbeds for crop establishment, manages weeds and crop residues, and incorporates fertilizers, manures, pesticides, and amendments into the soil (Srivastava *et al*., 2006). Traditionally, farms are prepared using energy-intensive ploughs, which cause rigorous loosening and inversion of topsoil. Modern conservation tillage systems are designed to minimise soil disturbance to conserve soil, water, and energy, besides ensuring crop residue retention on the field (FAO, 2014). Rotary tillage machines play a crucial role in realising conservation tillage since they can perform minimal soil manipulation in a single pass, thus eliminating the need for heavy machines (Yang *et al*., 2018; Matin *et al*., 2021). Rotary tillers have been widely adopted in rice-based farming due to their simplicity of use and ability to create finely-tilled and even seedbeds and incorporate crop residues into the soil (Ahmadi, 2017). However, conventional rotary tillers used for conservation tillage in intensive rice-based farming systems experience low efficiency due to the challenge of handling the degraded clayey-paddy-soils and working in extreme crop-residue cover conditions (Yang *et al*., 2019; Sirisak and Niyamapa, 2010). The blades often experience high resistance, lower soil and straw cutting efficiencies, and have high energy demands (Ahmad *et al*., 2017; Zhao *et al*., 2018). This causes poor seedbed quality, straws incorporation, and seeding machine clogging. Consequently, farmers end up performing time, energy, and cost-intensive rototilling of soil with up to 3-5 passes to achieve satisfactory seedbeds (Mottalib *et al*., 2019). In order to realise optimal conservation farming, there is a need for high-efficiency and energy-saving rotary tiller blade designs that are adaptable to the pervasive working conditions of the intensive rice-based rotational farming systems (Saimbhi *et al.,* 2004; Matin *et al*., 2021). The ideal rotary tillage blade should transfer maximum power from the rotor to the soil with minimal resistance and save on energy; produce the best tilth with good soil structure; break and incorporate residues into the soil; and prevent straws from coiling on the rotary shaft (Beeny and Khoo, 1970).

Researchers in the past focused on establishing the optimal shape of rotary tiller blades, and various design configurations were developed (Saimbhi *et al*., 2004). The commonly available rotary tiller blade designs include straight blades, L-shaped types, J-shaped blades, C-type blades, and twisted/curved blades (Yang *et al*., 2018). These designs have been constructed by simple alteration of the geometric shape of the blade. Biomimetics represents a viable approach to optimise the design of rotary tiller blades for conservation tillage. Biomimetics studies the well-adapted formations, structures, and biomechanical functionalities of living organisms and mimics them as prototypes for new engineering parts and/or systems. Biomimetic designs of cultivation tools are suggested to reduce resistance, enhance the structural strength of tools and improve working performance (Zhang *et al*., 2016; Yu *et al*., 2021).

Several researchers have employed biomimetics to develop and optimise soil-engaging tools. Tong *et al*. (2009) modelled the geometrical structures of the cuticle surfaces of a dung beetle (*Copris ochus* Motschulsky) on the surface of a tine furrow opener. The biomimetic furrow opener reduced stresses by up to 14.0% and power requirements by up to 28%. Zhang *et al*. (2018) developed a bionic imprinting toothed wheel based on the contour curve of the foreleg end of a dung beetle. They achieved up to a 16.5% reduction in draft forces and a 24.9% increase in the size of the imprinted micro basin. Ji *et al*. (2010) examined the curvature, and the derivative of the contour curve of the fore claw toes of a mole rat and uncovered that the claw structures presented perfect bionic prototypes for the design of soil cutting tools. Tong *et al*. (2015) developed biomimetic blades for soil-rototilling and stubble-breaking by learning from the geometrical structure of the tips of toes of a mole rat (*Scaptochirus moschatus)*. They realised that the biomimetic blades required lower torque than the universal blade. Yang *et al*. (2021) simulated the convex contour curves of the five claws of a mole rat on biomimetic rotary tiller blades. They revealed that the geometrical structure of the five foreclaws reduced the torque requirements during soil-cutting by up to 13.99%. With the apparent advantages that biomimetics presents to optimising tool designs in mechanised crop farming, it is crucial to explore the benefits of this concept in advancing conservation tillage technologies in the face of declining soil fertility and productivity in intensive farming systems. Therefore, the purpose of this study was to evaluate the operational performance and adaptability of biomimetically designed rotary tiller blades in realizing conservation tillage goals in intensive rice-based farming systems. The performances of the biomimetic rotary tiller blades were evaluated with regard to torque requirements, soil cutting and fragmentation characteristics, displacements of topsoil, and the rate of crop residue incorporation.

Materials and Methods

Design of the biomimetic rotary tiller blade

The biomimetic rotary tiller blade was developed by mimicking the geometrical structure of the toe claw of a mole rat (*Scaptochirus moschatus*), which has been established to possess high soil digging efficiency (Ji *et al*., 2010; Tong *et al*., 2015). Following the work of Tong *et al*. (2015), the arch-shape of the middle claw toe was replicated on the curved scooping edges of a conventional blade to form the biomimetic rotary tillage blade. As a result, five concave arcs were created and equally arranged on the curved cutting edges, as shown in Figure 1. The bionic arcs had a distance of 20 mm between the crests and 8 mm deep.

The performance of the biomimetic rotary tiller blade was compared to that of an equivalent conventional blade. Both blades were made of high carbon steel, had a thickness of 6 mm, an operational radius of 208 mm, and a single-blade working width of 45 mm. Properties of soil samples collected from the experimentation field were determined. The samples were composed of 37.56 % sand (>0.2 mm), 40.24 % silt (0.2-0.002), and 22.10 % clay (<0.002 mm); and classified as clay-loam, according to USDA soil taxonomy (ASTM, 2017). Cylindrical soil cores (50 mm in diameter and 50 mm in length) were collected randomly from 15 locations and three depths of 50, 100, and 150 mm, and three samples at each depth. The soil samples were weighed before and after oven-drying at 105°C for 24 h and used to determine soil bulk density and moisture content (dry basis) (Carter and Gregorich, 2008). Soil cone-index was measured at 15 random locations in the field to a depth of 150 mm using a digital cone-penetrometer (TJSD-750-IV Zhejiang TOP Agricultural Technology Co., China) (ASABE, 2006). Soil cohesion and internal friction angle were determined

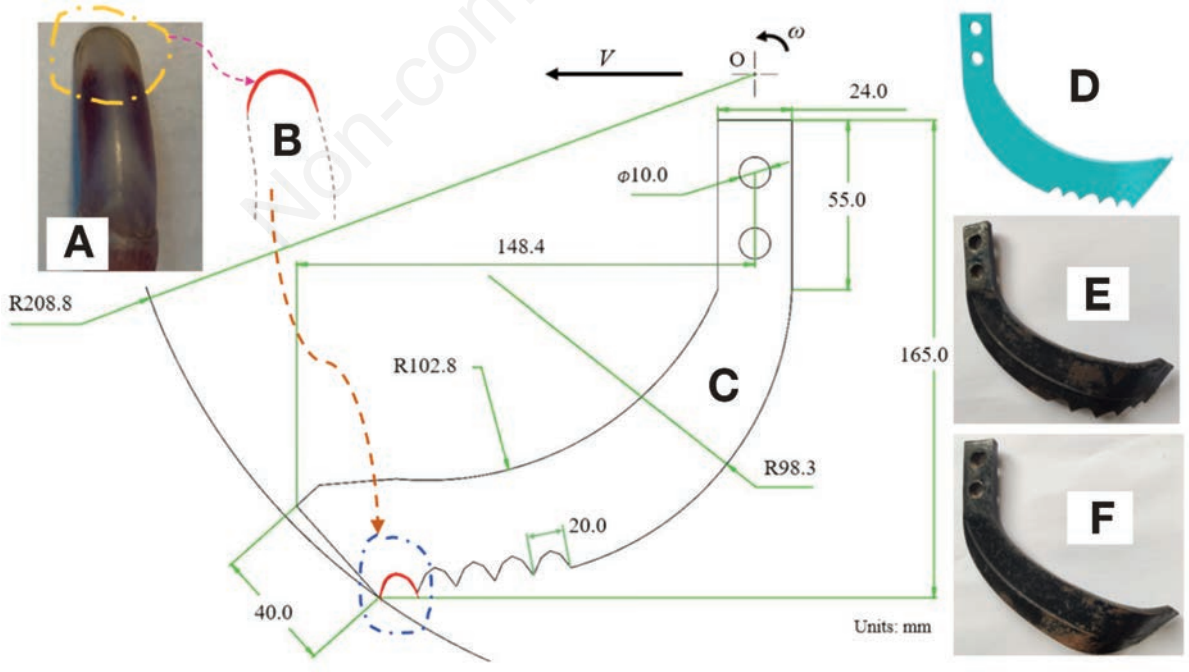

Figure 1. A) Toe claw of the mole rat (*Scaptochirus moschatus*) (Tong *et al*., 2015); B) geometric outline of the mole's toe-claw (Yang *et al*., 2021); C) configurations of the biomimetic rotary tiller blade; D) 3D impression of the biomimetic tiller blade; E) modified bionic rotary tiller blade; F) conventional curved rotary tillage blade.

using direct shear box apparatus (Fredlund and Vanapalli, 2002). The soil properties were as summarised in Table 1.

Field experimental setup

Experiments were conducted in an experimentation farm located in Luhe District, Nanjing, China (32°25'53.4" N, 118°55'51.0" E), using a multi-functional in-situ test-rig facility developed at Nanjing Agricultural University. The test rig measured 8m long by 1.8m wide and stood on steel wheels resting on rails that allowed its mobility across experimental plots. It was powered by a 13.5 kW generator and consisted of a tool-carriage unit, a 4-kW traction motor, chain drives, depth adjustment motors, power & data transmission cables, and force sensors. The setup was as shown in Figure 2.

Experimental design

A flat portion of dry ground on the field was cleared of surface cover and divided into 6 rectangular plots (of 6 m by 2 m). Twelve rotary tiller blades, spanning a width of 500 mm, were fastened onto the rotor shaft of the tool carriage. The rotary tiller blades were then driven through a ground distance of 3 m, at a constant

Table 1. Soil mechanical properties.

Parameter	Value
Soil bulk density, γ (Mg m^{-3})	1.398
Cohesion, c (kPa)	40.52
Soil moisture content, % (dry basis)	22.90
Young's modulus, E (MPa)	2.84
Poisson's ratio, υ	0.43
Coefficient of soil-metal friction, μ	0.42
Internal friction angle (°)	12.90
Soil cone index, (kPa)	795.00

Figure 2. Setup of the test-rig platform: 1- height adjustment motor, 2- control panel, 3- power connection, 4- data cable, 5- rail, 6- traction motor, 7- data acquisition computer, 8- portable generator, 9- Advantech data acquisition module, 10- mudguard, 11- rotary shaft, 12- bionic rotary tiller blade, 13- tool holder, 14- rotary shaft motor, 15- assembled experimental rotavator, and 16- drawing chains.

forward speed of 0.1 m s^{-1} and rotational speed of 300 rpm. Tillage depth was varied at 40, 70, and 100 mm, and each test was replicated three times in a randomised block design.

The torque on the rotary shaft was measured in real-time using calibrated torque transducer mounted on the shaft transmission mechanism. Data acquisition was made using LabVIEW2010 software (National Instruments Corporation, Austin, TX, USA), interfaced with Advantech portable module USB-4704-AE (Advantech Co., Ltd, Taipei, Taiwan). Acquired data were saved to a laptop in LabVIEW measurement format (LVM), at a rate of 500 Hz and later converted to MS-Excel spreadsheets for processing.

From the measured values of torque in each case, the specific work requirements of the rotary tiller blades were calculated using the equation below (Matin *et al.,* 2015).

$$Specific\ work\ (kJ\ m^3) = \frac{T \times N \times \pi}{30 \times V \times b \times h} \quad (1)$$

where T is torque (kN.m), N is the rotational velocity (rpm), V is the forward velocity (m s^{-1}), b is the working width (m), and h is the tillage depth (m). To determine the vertical displacements and rate of soil mixing within the tilth layer, ten small square plastics (15 mm by 15 mm), marked 1-10 were used (Figure 3A). The tracers were aligned evenly across the path of rotary tillage. After the ground had been tilled, tracers on the surface were identified while a trowel was used to dig up tracers buried in the soil, and then their depth was measured.

The rate of crop-residue incorporation into the soil was estimated using coloured straws (Figure 3A). Straws (of an average length of 150 mm) were spray-painted with distinct colours (*i.e.*, red and green), marked, and then placed along the path of tool travel. Red-coloured straws were placed parallel to the tillage direction, while the green straws were placed perpendicular to the tillage direction. There were 18 stalks in each set. After each test, the coloured straws (both cut and uncut) present on the surface were collected. The amount of straw collected was subtracted from the original amount initially applied on the surface and used to calculate the rate of straw incorporation, S_i, as in Eq. 2.

$$S_i = \frac{N_o - N_s}{N_o} \times 100\% \quad (2)$$

where N_o is the initial amount of straws before rotary tillage while, N_s is the amount of marked straws on the surface.

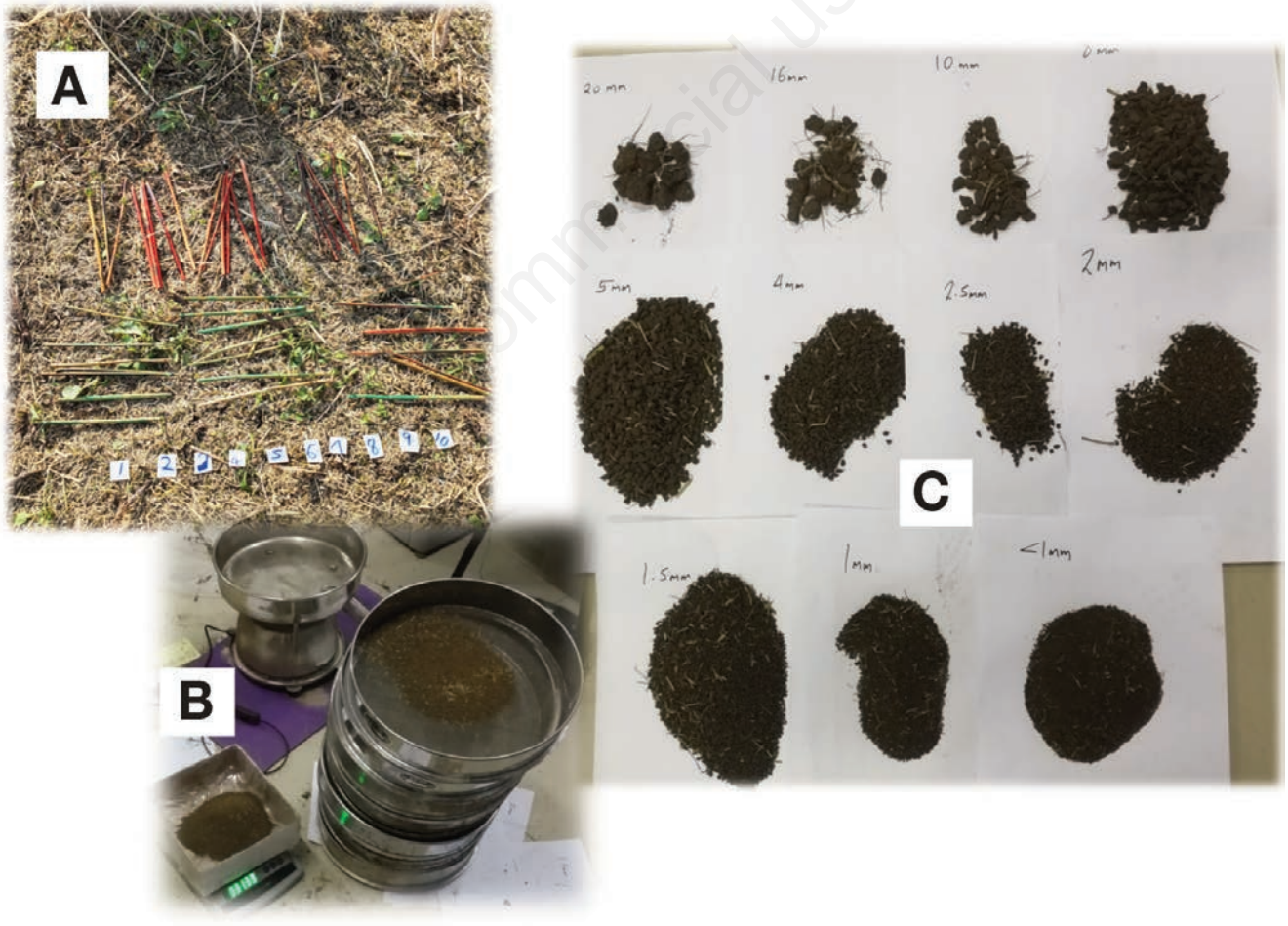

Figure 3. A) Plastic and coloured straw tracers (red and green) were used to determine soil displacements and the rate of straw incorporation; B) vibrating shaker sieving machine for determining soil clod sizes; C) sieved soil and categorised into different aggregate sizes.

To determine the soil cutting effects and the distribution of soil clod aggregate sizes after tillage, dry sieve analysis was performed on three soil samples randomly collected from each replication. First, equal proportions (1000 grams) of soil were weighed, and each stratified into ten aggregate sizes (*i.e.*, >20, 16-20, 10-16, 8-10, 5-8, 4-5, 3-4, 2-3, 1-2, and <1 mm) using a vibrating shaker stacked with wire sieves containing progressively smaller openings from top to bottom (Figure 3B). The mass of soil aggregates retained on each sieve was determined and expressed as a percentage of the total dry weight in each case. The ratios were calculated using Eq. 3.

$$\%\ Soil\ particles\ retained = \frac{weight\ of\ soil\ retained}{total\ weight\ of\ sample} \times 100\% \quad (3)$$

From the proportions of soil clod sizes, dry mean weight diameters MWD was calculated to establish the extent and nature of soil disintegration by tillage loads. MWD was calculated as Eq. 4 (Kemper and Rosenau, 1986).

$$MWD = \sum_{i=1}^{n} \bar{x}_i . W_i \quad (4)$$

where $\bar{x}_i$ is the mean diameter of each aggregate size, W_i is the proportion of total sample weight in the corresponding aggregate size, while n is the number of fractions into which the soil is graded.

Data analysis

Statistical analysis was performed using IBM-SPSS Statistics 22 software (IBM Corp., Armonk, N.Y., USA) at a 95% confidence interval. Levene's test for equality of variances revealed heterogeneity within-group variances; therefore, Brown-Forsythe test (F*-test ANOVA) with Games-Howel post hoc tests of 'equal variances not assumed' was used to determine the effects of changing tillage depth on the measured torque. Independent samples t-tests were used to compare the torque values recorded by the individual rotary tiller blades. Descriptive statistics, percentages, and absolute values were used to describe the characteristics of soil mixing, straw incorporation, and soil particle sizes.

Results and Discussion

Torque and power requirements

The conventional rotary tiller blades registered higher mean torque values than the biomimetic blades. Independent samples t-tests used to compare the performance of the two designs revealed statistically significant differences in their mean scores at all tillage depths. At the 40 mm depth, the scores were: t (3996.691)=7.046, P<0.05, with the bionic blades having (M=24.9458, SD=9.57109) while the conventional blades had (M=27.0981, SD=9.74590). At 70 mm depth, the scores were: t (3682.047)=20.723, P<0.05, with the bionic blades having (M=42.0972, SD=11.37048) while the conventional blades had (M=50.9588, SD=15.37573). At 100 mm depth, the scores were: t (2647.180)=9.829, P<0.05, with the bionic designs having (M=56.8470, SD=13.44435) while the conventional blades had (M=64.6655, SD=32.93568).

The performance of the two designs was as plotted in Figure 4.

The biomimetic blades minimised torque by 8.63%, 21.05%, and 13.75% at the 40, 70, and 100 mm depths, respectively, compared to the conventional blades. This corroborates the earlier findings of Tong *et al.* (2015), who experimented on a similar design and postulated that increasing the number of bionic features on the tiller blades would further improve the working efficacy.

The mean torque values recorded from both rotary tiller blade designs increased with tillage depth. F*-test ANOVA revealed that changing the tillage depth significantly affected the loads experienced on the rotary shaft. The statistics for the conventional tiller blades were: F(2, 3228.846)=1531.270, P<0.05; while the statistics of the biomimetic rotary tiller blades were: F(2, 5581.299)=3807.884, P<0.05. Post hoc comparisons using the Games-Howell test indicated that the mean scores of both blades were significantly different across all three tillage depths.

Analysis of the energy demands of the rotary blades revealed that the bionic design had lower power requirements than the conventional design. This was evident with the bionic blade registering lower specific work values at all the three tillage depths, as seen in Figure 5.

During soil engagement, the curves and crests on the biomimetic rotary tiller blades enhanced penetration and cutting into the soil with minimal resistance, thus the reduced torque and specific power requirements. Similar observations were made by Yang *et al*. (2021), who experimented on a blade with simulated five profile curves of the mole rat's claws. In addition, the bionic modifications on the tool improved stress distribution on the soil cutting surfaces, thus optimising its structural capability (Guo *et al*., 2009).

The specific work of the rotary tiller is a derivative of the work carried out by the tool during each rotation of blades per the volume of broken soil. The analysis gives a more precise prediction of the tools' performance since it considers the influence of the working speed and working depth (Matin *et al.*, 2015). In this case, it was evident that the bionic blade was more energy-efficient as it

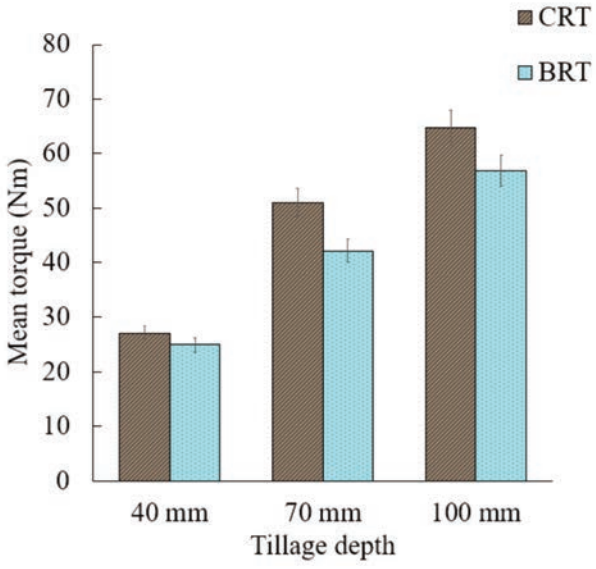

Figure 4. Mean torque was measured from the biomimetic rotary tiller (BRT) blade compared to the conventional (CRT) blade at the three tillage depths.

had less specific work requirements and thus optimised for economical tillage. Reduced power requirements will improve the working rate and enable the use of light-duty tractors and lighter machine parts (Zhu and Chen, 2013). Achieving lighter machines would allow for the design of multi-functional implements which would combine several field operations, thus minimising the number of farm passes; consequently saving on energy, labour costs, and turnaround time, besides minimising soil compaction (Srivastava *et al*., 2006; Zhang *et al*., 2016).

Rate of soil displacement

Tracer displacements and distribution in the soil were used to estimate the tool's ability to mix upper and lower soil layers during tillage. Out of the ten pieces, the tracers found on the surface for the conventional rotary tiller blades were 7, 5, and 4 for tests at the 40, 70, and 100 mm depths, respectively. The biomimetic blades buried more tracers, with only 4, 3, and 2 tracers found on the surface at three depths.

Table 2 below summarises the vertical displacements and distribution of tracers by the rotary tiller blades

The biomimetic blades displaced the tracers furthest into the soil with higher maximum depths of 2.9, 6.2, and 8.6 cm at the 40, 70, and 100 mm working depths, respectively, compared to 2.2, 5.2, and 7.7 cm of the conventional blades. The improved soil displacement capability would enable the biomimetic blades to achieve more disturbance that would be useful in breaking plough pans and tough clods. This will, in turn, improve soil aeration, water infiltration, mixing of fertilisers and soil, root development space, and the quality of seedbeds (Celik *et al*., 2008; Yao *et al*., 2015).

Straw incorporation performance

The number of coloured straws collected on the surface after tillage was used to estimate the tools' rate of straw incorporation into the soil tilth. Figure 6 below summarises the rates of straw burial by the two rotary tiller blades at the three tillage depths.

The rate of straw burial increased with tillage depth. The perpendicularly aligned straws were buried more than those positioned parallel to the tillage direction. The biomimetic rotary tiller blades generally had higher rates of straw burial than the conventional design, with the highest difference being 12.5% when working at 70 mm depth in both arrangements. Therefore, the curved cutting surfaces of the bionic modifications optimised the blades' straw cutting and incorporation capability. This would enhance the handling of the excessive crop residues generated after the farming seasons and would minimise the coiling of straws around the blades during seeding, thus creating better and smoother machine operation. Moreover, with the improved straw incorporation and better soil mixing rate, decomposition, and nutrients cycling would be enhanced, increasing the utility of the crop residues and improving soil fertility and productivity. This advantage contributes to the realisation of conservation tillage in intensive farming systems (Matin *et al*., 2021).

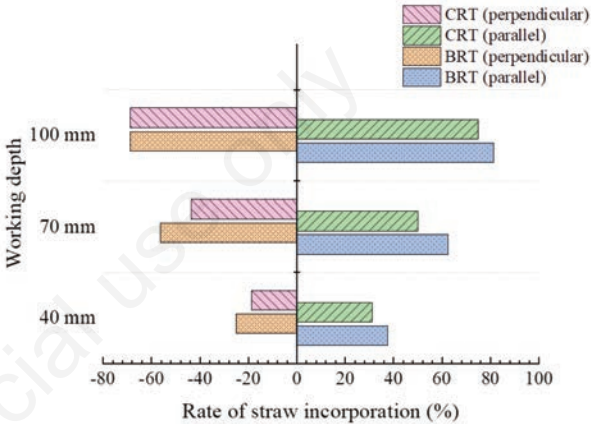

Figure 6. Straw incorporation rates of the biomimetic rotary tiller (BRT) blades and the conventional (CRT) blades (The (-) sign is used to indicate displacements of perpendicularly arranged straws while positive represents displacements of parallelly aligned straws).

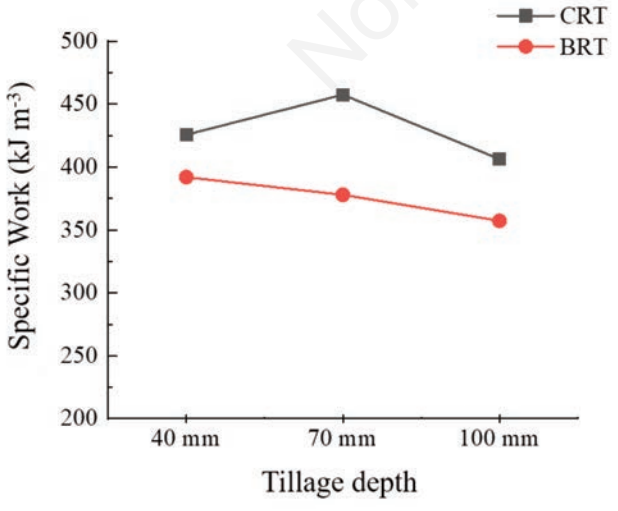

Figure 5. Specific work requirements of the bionic (BRT) and the conventional rotary tiller (CRT) blades at the three tillage depths.

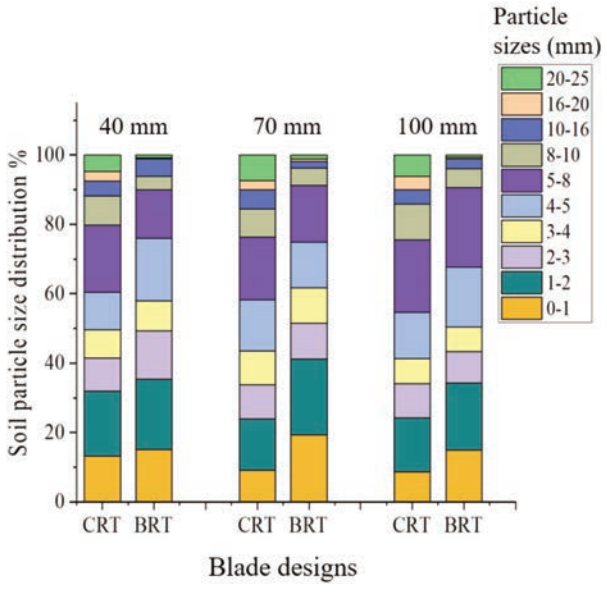

Figure 7. Distribution of soil aggregate sizes after tillage using the conventional rotary tiller blades (CRT) and biomimetic blades (BRT).

Soil cutting characteristics and particle size analysis

The soil aggregates due to rototilling were graded into the various categories of clod sizes retained on each sieve after particle size analysis. The distribution of the aggregate sizes over the total dry weight of soil sieved was as plotted in Figure 7.

The biomimetic blades produced smaller particles than the conventional blades, as indicated by the more significant proportions in the smaller aggregate sizes.

Mean weight diameter (MWD) clearly portrayed the biomimetic rotary tiller blades' soil cutting and failure behaviour (Liu *et al*., 2019). The MWDs of the two blades and the clod sizes at the three tillage depths were summarised in Figure 8.

The differences in the MWD indicate that the two designs had distinct soil failure properties. The clod sizes from both designs increased with working depth. However, the MWD values of the biomimetic blades were much lower and spread over a small range of 0.47 mm between the highest and lowest tillage depths, whereas the conventional design had higher MWD values with a range of 0.8 mm. It was thus clear that the biomimetic blade designs generated much finer tilth with granular and more even soil clod sizes than the conventional blades and thus improved soil fragmentation ability. These observations agree with Yang *et al*. (2019), who showed that a functional combination of all the mole rat's claws had a smaller soil failure wedge with a rupture ratio of 19.6% less than normal.

On the other hand, Saimbhi *et al*. (2004) revealed that the conventional rotary tiller blades engaged soil with slide-cutting action that tends to cause compactions on the flat underside of the blade. This slide-cutting action produced larger and irregularly shaped clods with a platy structure, as observed in our analysis (Figure 8). Therefore, by employing the biomimetic design adopted from the claw structure of the mole rat, the slide cutting and compaction of the conventional rotary tiller blades are minimised. This will improve the soil structure faster, thus avoiding the need for multiple tillage passes to achieve satisfactory tilth and lower power requirements. Furthermore, achieving granular and finer soil struc-

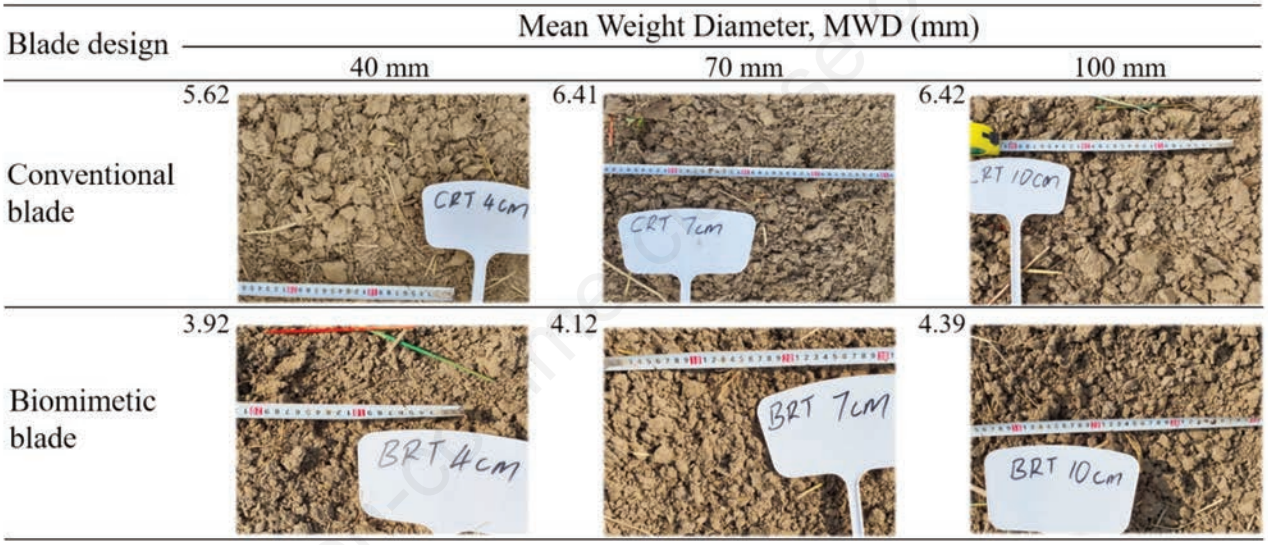

Figure 8. Mean weight diameter (MWD) and tillage effects of the biomimetic rotary tiller blades compared to conventional blades.

Table 2. Vertical displacements and distribution of the tracers in the soil tilth.

Tracer designation	Depth of tracers in tilled soil (cm)					
	40 mm depth		70 mm depth		100 mm depth	
	CRT	BRT	CRT	BRT	CRT	BRT
1	0	0	2.9	3.6	6.4	5
2	0	1.4	0	5.2	0	4.8
3	0	2.7	0	0	7.7	0
4	1.9	2.9	5.2	6.2	0	4.3
5	0	0	4.7	4.3	4.4	8.6
6	0	0	0	5	0	5.8
7	0	3.5	0.3	0	4.7	4
8	2.2	1.9	0	4.7	0	6.6
9	1.5	2.6	3	0	5.2	0
10	0	0	0	5.6	3.8	3.7

CRT, conventional rotary tiller blades; BRT, biomimetic rotary tiller blades.

ture will improve seedbed quality with better water infiltration and retention, soil strength, pore size distribution, and aeration (Srivastava *et al*., 2006). This will be particularly instrumental in removing soils and creating conducive crop growing conditions in the intensive rice-wheat crop rotation farming, where highly compacted and degraded soil structure due to puddling and anaerobic conditions needs to be rehabilitated for guaranteed crop yield (Yao *et al*., 2015).

Conclusions

Field experiments were conducted to evaluate the performance of biomimetic rotary tiller blades that mimic the geometrical structure of the mole rat's claw. Torque and specific power requirements, soil fragmentation, displacement characteristics, and straw incorporation performance of the biomimetic blades were compared to those of conventional blades at three tillage depths. The study revealed that the biomimetic rotary tiller blades enhanced soil cutting and significantly reduced torque on the rotary shaft by up to 21.05%, lowered specific power requirements, and produced finer tilths with granular and more even soil clod sizes. They also improved the redistribution of topsoil and straw incorporation. Therefore, the biomimetic rotary tiller blades are energy-efficient and can improve the quality of seedbeds in a single-pass field operation, besides enhancing straw management. Therefore, biomimetic designs of rotary tiller blades present an opportunity to optimise the operational performance of rotary tiller blades and contribute to the implementation of minimal conservation tillage in intensive farming systems. In future work on bionic designs for optimised soil-engaging tools, there is a need for in-depth study on appropriate biomimetic materials and design approaches such as bionic electro-osmosis to develop bio-inspired working surfaces. Furthermore, there is a great protentional application of bionic designs in intelligent and automated farm machinery by simulating the perception mechanism and bio-receptors of external stimuli such as changes in working environments and improving machine stability and precision.

References

Ahmad F., Ding W., Ding Q., Rehim A., Khawar J. 2017. Comparative performance of various disc-type furrow openers in no-till paddy field conditions. Sustainability. 9:1-15.

Ahmadi I. 2017. A torque calculator for rotary tiller using the laws of classical mechanics. Soil Till. Res. 165:137-43.

ASABE. 2006. Soil cone penetrometer. In: ASAE Standards American Society of Agricultural & Biological Engineers. ASAE S313.3.

ASTM. 2017. Standard Practice for Classification of Soils for Engineering Purposes (Unified Soil Classification System). ASTM International. ASTM D2487-17.

Beeny J.M., Khoo D.C.P. 1970. Preliminary investigations into the performance of different shaped blades for the rotary tillage of wet rice soil. J. Agr. Eng. Res. 15:27-33.

Carter M.R., Gregorich E.G. 2008. Soil sampling and methods of analysis (2nd ed.). CRC Press, Taylor & Francis Group, Boca Raton, FL, USA.

Celik A., Ozturk I., Way T.R. 2008. A theoretical approach for determining irregularities of the bottom of the tillage layer caused by horizontal axis rotary tillers. Agric. Eng. Int. CIGR J. 9:1-9.

FAO. 2014. Conservation agriculture: The 3 principles. Conservation Agriculture: The 3 Principles. Food and Agriculture Organization. Available from: https://www.fao.org/conservation-agriculture/en/ Accessed: 17 September, 2021.

Fredlund D., Vanapalli S. 2002. Shear strength of unsaturated soils. In: J. H. Dane & G. C. Topp (Eds.), Methods of soil analysis: Part 4 - Physical methods. Soil Science Society of America. 5:329-361.

Guo Z., Zhou Z., Zhang Y., Li Z. 2009. Bionic optimization research of soil cultivating component design. Sci. China Ser. E-Technol. Sci. 52:955-65.

Ji W.F., Chen D.H., Jia H.L., Tong J. 2010. Experimental investigation into soil-cutting performance of the claws of mole rat (Scaptochirus moschatus). Wear. 7:S166-71.

Kemper W.D., Rosenau R.C. 1986. Aggregate stability and size distribution. In: A. Klute (Ed.), Methods of soil analysis: Part I. Physical and mineralogical methods, 2nd ed. Agronomy, pp 425-442.

Liu M., Han G., Zhang Q. 2019. Effects of soil aggregate stability on soil organic carbon and nitrogen under land use change in an erodible region in southwest China. Int. J. Env. Res. Pub. He. 16:3809.

Matin, Md. A., Fielke, J.M., Desbiolles, J.M.A. 2015. Torque and energy characteristics for strip-tillage cultivation when cutting furrows using three designs of rotary blade. Biosyst. Eng. 129:329-40.

Matin Md. A., Hossain M.I, Gathala M.K., Timsina J., Krupnik T.J. 2021. Optimal design and setting of rotary strip-tiller blades to intensify dry season cropping in Asian wet clay soil conditions. Soil Till. Res. 207:104854.

Mottalib M.A., Hossain M.A., Hossain M.I., Amin M.N., Alam M.M., Saha C.K. 2019. Assessment of cost-benefit parameters of conservation agricultural machinery for custom hires entrepreneurship in the southern region of Bangladesh. Agric. Eng. Int. CIGR J. 21:94-103.

Saimbhi V., Wadhwa D., Grewal P. 2004. Development of rotary tiller blade using three-dimensional computer graphic. Biosyst. Eng. 89:47-58.

Sirisak C., Niyamapa T. 2010. Variations of torque and specific tilling energy for different rotary blades. Int. Agric. Eng. J. 19:1-14.

Srivastava A.K., Goering C.E., Rohrbach R.P., Buckmaster D.R. 2006. Engineering principles of agricultural machines (2nd Ed.). American Society of Agricultural and Biological Engineers.

Tong J., Moayad B.Z., Ma Y., Sun J., Chen D., Jia H., Ren L. 2009. Effects of biomimetic surface on designs on furrow opener performance. J. Bionic Eng. 6:280-9.

Tong J., Ji W., Jia H., Chen D., Yang X. 2015. Design and tests of biomimetic blades for soil-rototilling and stubble-breaking. J. Bionic Eng. 12:495-503.

Yang Y., Fielke J., Ding Q., He R. 2018. Field experimental study on optimal design of the rotary strip-till tools applied in rice-wheat rotation cropping system. Int. J. Agric. Biol. Eng. 11:88-94.

Yang Y., Li M., Tong J., Ma Y. 2018. Study on the interaction between soil and the five-claw combination of a mole using the Discrete Element Method. Appl. Bionics Biomech. 1-11.

Yang Y., Tong J., Huang Y., Li J., Jiang X. 2021. Biomimetic rotary tillage blade design for reduced torque and energy requirement. Appl. Bionics Biomech. 1-16.

Yang Y., Tong J., Ma Y., Jiang X., Li J. 2019. Design and experiment of biomimetic rotary tillage blade based on multiple claws

characteristics of mole rats. Trans. Chin. Soc. Agric. Eng. 35:37-45.
Yao S., Teng X., Zhang B. 2015. Effects of rice straw incorporation and tillage depth on soil puddlability and mechanical properties during rice growth period. Soil Till. Res. 146(Part B):125-32.
Yu H., Han Z., Zhang J., Zhang S. 2021. Bionic design of tools in cutting: reducing adhesion, abrasion or friction. Wear. 203955:482-3.
Zhang Z.J., Jia H.L., Sun J.Y. 2016. Review on application of biomimetic for designing soil-engaging tillage implements in Northeast China. Int. J. Agric. Biol. Eng. 9:12-21.
Zhang Z., Wang X., Tong J., Carr S. 2018. Innovative design and performance evaluation of bionic imprinting toothed wheel. Appl. Bionics Biomech. 9806287.
Zhao H.B., He J., Li H.W., Mao Y.J., Hu H.N., Zhang Z.Q., Liu P. 2018. Comparison on soil, straw disturbance and resistance of conventional and plain-straight blade for strip-tillage with Discrete Element Method. Int. Agric. Eng. J. 27:229-40.
Zhu W., Chen C. 2013. Bionics design of stubble blade based on the digging claw of mole cricket. Appl. Mech. Mater. 397:775-8.